

Y Production in $p\bar{p}$ Collisions at $\sqrt{s} = 1.8$ TeV

- F. Abe,¹³ M. G. Albrow,⁷ S. R. Amendolia,²² D. Amidei,¹⁶ J. Antos,²⁸ C. Anway-Wiese,⁴ G. Apollinari,²⁶ H. Areti,⁷ M. Atac,⁷ P. Auchincloss,²⁵ F. Azfar,²¹ P. Azzi,²⁰ N. Bacchetta,²⁰ W. Badgett,¹⁶ M. W. Bailey,¹⁸ J. Bao,³⁵ P. de Barbaro,²⁵ A. Barbaro-Galtieri,¹⁴ V. E. Barnes,²⁴ B. A. Barnett,¹² P. Bartalini,²² G. Bauer,¹⁵ T. Baumann,⁹ F. Bedeschi,²² S. Behrends,³ S. Belforte,²² G. Bellettini,²² J. Bellinger,³⁴ D. Benjamin,³¹ J. Benloch,¹⁵ J. Bensinger,³ D. Benton,²¹ A. Beretvas,⁷ J. P. Berge,⁷ S. Bertolucci,⁸ A. Bhatti,²⁶ K. Biery,¹¹ M. Binkley,⁷ F. Bird,²⁹ D. Bisello,²⁰ R. E. Blair,¹ C. Blocker,³ A. Bodek,²⁵ W. Bokhari,¹⁵ V. Bolognesi,²² D. Bortoletto,²⁴ C. Boswell,¹² T. Boulos,¹⁴ G. Brandenburg,⁹ C. Bromberg,¹⁷ E. Buckley-Geer,⁷ H. S. Budd,²⁵ K. Burkett,¹⁶ G. Busetto,²⁰ A. Byon-Wagner,⁷ K. L. Byrum,¹ J. Cammerata,¹² C. Campagnari,⁷ M. Campbell,¹⁶ A. Caner,⁷ W. Carithers,¹⁴ D. Carlsmith,³⁴ A. Castro,²⁰ Y. Cen,²¹ F. Cervelli,²² H. Y. Chao,²⁸ J. Chapman,¹⁶ M.-T. Cheng,²⁸ G. Chiarelli,²² T. Chikamatsu,³² C. N. Chiou,²⁸ L. Christofek,¹⁰ S. Cihangir,⁷ A. G. Clark,²² M. Cobal,²² M. Contreras,⁵ J. Conway,²⁷ J. Cooper,⁷ M. Cordelli,⁸ C. Couyoumtzelis,²² D. Crane,¹ J. D. Cunningham,³ T. Daniels,¹⁵ F. DeJongh,⁷ S. Delchamps,⁷ S. Dell'Agnello,²² M. Dell'Orso,²² L. Demortier,²⁶ B. Denby,²² M. Deninno,² P. F. Derwent,¹⁶ T. Devlin,²⁷ M. Dickson,²⁵ J. R. Dittmann,⁶ S. Donati,²² R. B. Drucker,¹⁴ A. Dunn,¹⁶ K. Einsweiler,¹⁴ J. E. Elias,⁷ R. Ely,¹⁴ E. Engels, Jr.,²³ S. Eno,⁵ D. Errede,¹⁰ S. Errede,¹⁰ Q. Fan,²⁵ B. Farhat,¹⁵ I. Fiori,² B. Flaughner,⁷ G. W. Foster,⁷ M. Franklin,⁹ M. Frautschi,¹⁸ J. Freeman,⁷ J. Friedman,¹⁵ H. Frisch,⁵ A. Fry,²⁹ T. A. Fuess,¹ Y. Fukui,¹³ S. Funaki,³² G. Gagliardi,²² S. Galeotti,²² M. Gallinaro,²⁰ A. F. Garfinkel,²⁴ S. Geer,⁷ D. W. Gerdes,¹⁶ P. Giannetti,²² N. Giokaris,²⁶ P. Giromini,⁸ L. Gladney,²¹ D. Glenzinski,¹² M. Gold,¹⁸ J. Gonzalez,²¹ A. Gordon,⁹ A. T. Goshaw,⁶ K. Goulios,²⁶ H. Grassmann,⁶ A. Grewal,²¹ L. Groer,²⁷ C. Grosso-Pilcher,⁵ C. Haber,¹⁴ S. R. Hahn,⁷ R. Hamilton,⁹ R. Handler,³⁴ R. M. Hans,³⁵ K. Hara,³² B. Harral,²¹ R. M. Harris,⁷ S. A. Hauger,⁶ J. Hauser,⁴ C. Hawk,²⁷ J. Heinrich,²¹ D. Cronin-Hennessy,⁶ R. Hollebeck,²¹ L. Holloway,¹⁰ A. Hölscher,¹¹ S. Hong,¹⁶ G. Houk,²¹ P. Hu,²³ B. T. Huffman,²³ R. Hughes,²⁵ P. Hurst,⁹ J. Huston,¹⁷ J. Huth,⁹ J. Huyen,⁷ M. Incagli,²² J. Incandela,⁷ H. Iso,³² H. Jensen,⁷ C. P. Jessop,⁹ U. Joshi,⁷ R. W. Kadel,¹⁴ E. Kajfasz,^{7,*} T. Kamon,³⁰ T. Kaneko,³² D. A. Kardelis,¹⁰ H. Kasha,³⁵ Y. Kato,¹⁹ L. Keeble,⁸ R. D. Kennedy,²⁷ R. Kephart,⁷ P. Kesten,¹⁴ D. Kestenbaum,⁹ R. M. Keup,¹⁰ H. Keutelian,⁷ F. Keyvan,⁴ D. H. Kim,⁷ H. S. Kim,¹¹ S. B. Kim,¹⁶ S. H. Kim,³² Y. K. Kim,¹⁴ L. Kirsch,³ P. Koehn,²⁵ K. Kondo,³² J. Konigsberg,⁹ S. Kopp,⁵ K. Kordas,¹¹ W. Koska,⁷ E. Kovacs,^{7,*} W. Kowald,⁶ M. Krasberg,¹⁶ J. Kroll,⁷ M. Kruse,²⁴ S. E. Kuhlmann,¹ E. Kuns,²⁷ A. T. Laasanen,²⁴ N. Labanca,²² S. Lammel,⁴ J. I. Lamoureux,³ T. LeCompte,¹⁰ S. Leone,²² J. D. Lewis,⁷ P. Limon,⁷ M. Lindgren,⁴ T. M. Liss,¹⁰ N. Lockyer,²¹ C. Loomis,²⁷ O. Long,²¹ M. Loreti,²⁰ E. H. Low,²¹ J. Lu,³⁰ D. Lucchesi,²² C. B. Luchini,¹⁰ P. Lukens,⁷ J. Lys,¹⁴ P. Maas,³⁴ K. Maeshima,⁷ A. Maghakian,²⁶ P. Maksimovic,¹⁵ M. Mangano,²² J. Mansour,¹⁷ M. Mariotti,²⁰ J. P. Marriner,⁷ A. Martin,¹⁰ J. A. J. Matthews,¹⁸ R. Mattingly,¹⁸ P. McIntyre,³⁰ P. Melese,²⁶ A. Menzione,²² E. Meschi,²² G. Michail,⁹ S. Mikamo,¹³ M. Miller,⁵ R. Miller,¹⁷ T. Mimashi,³² S. Miscetti,⁸ M. Mishina,¹³ H. Mitsushio,³² S. Miyashita,³² Y. Morita,³² S. Moulding,²⁶ J. Mueller,²⁷ A. Mukherjee,⁷ T. Muller,⁴ P. Musgrave,¹¹ L. F. Nakae,²⁹ I. Nakano,³² C. Nelson,⁷ D. Neuberger,⁴ C. Newman-Holmes,⁷ L. Nodulman,¹ S. Ogawa,³² S. H. Oh,⁶ K. E. Ohl,³⁵ R. Oishi,³² T. Okusawa,¹⁹ C. Pagliarone,²² R. Paoletti,²² V. Papadimitriou,³¹ S. P. Pappas,³⁵ S. Park,⁷ J. Patrick,⁷ G. Pauletta,²² M. Paulini,¹⁴ L. Pescara,²⁰ M. D. Peters,¹⁴ T. J. Phillips,⁶ G. Piacentino,² M. Pillai,²⁵ R. Plunkett,⁷ L. Pondrom,³⁴ N. Produit,¹⁴ J. Proudfoot,¹ F. Ptohos,⁹ G. Punzi,²² K. Ragan,¹¹ F. Rimondi,² L. Ristori,²² M. Roach-Bellino,³³ W. J. Robertson,⁶ T. Rodrigo,⁷ J. Romano,⁵ L. Rosenson,¹⁵ W. K. Sakumoto,²⁵ D. Saltzberg,⁵ A. Sansoni,⁸ V. Scarpine,³⁰ A. Schindler,¹⁴ P. Schlabach,⁹ E. E. Schmidt,⁷ M. P. Schmidt,³⁵ O. Schneider,¹⁴ G. F. Sciacca,²² A. Scribano,²² S. Segler,⁷ S. Seidel,¹⁸ Y. Seiya,³² G. Sganos,¹¹ A. Sgolacchia,² M. Shapiro,¹⁴ N. M. Shaw,²⁴ Q. Shen,²⁴ P. F. Shepard,²³ M. Shimojima,³² M. Shochet,⁵ J. Siegrist,²⁹ A. Sill,³¹ P. Sinervo,¹¹ P. Singh,²³ J. Skarha,¹² K. Sliwa,³³ D. A. Smith,²² F. D. Snider,¹² L. Song,⁷ T. Song,¹⁶ J. Spalding,⁷ L. Spiegel,⁷ P. Sphicas,¹⁵ L. Stanco,²⁰ J. Steele,³⁴ A. Stefanini,²² K. Strahl,¹¹ J. Strait,⁷ D. Stuart,⁷ G. Sullivan,⁵ K. Sumorok,¹⁵ R. L. Swartz Jr.,¹⁰ T. Takahashi,¹⁹ K. Takikawa,³² F. Tartarelli,²² W. Taylor,¹¹ P. K. Teng,²⁸ Y. Teramoto,¹⁹ S. Tether,¹⁵ D. Theriot,⁷ J. Thomas,²⁹ T. L. Thomas,¹⁸ R. Thun,¹⁶ M. Timko,³³ P. Tipton,²⁵ A. Titov,²⁶ S. Tkaczyk,⁷ K. Tollefson,²⁵ A. Tollestrup,⁷ J. Tonnison,²⁴ J. F. de Troconiz,⁹ J. Tseng,¹² M. Turcotte,²⁹ N. Turini,²² N. Uemura,³² F. Ukegawa,²¹ G. Unal,²¹ S. C. van den Brink,²³ S. Vejcek III,¹⁶ R. Vidal,⁷ M. Vondracek,¹⁰ D. Vucinic,¹⁵ R. G. Wagner,¹ R. L. Wagner,⁷ N. Wainer,⁷ R. C. Walker,²⁵ C. Wang,⁶ C. H. Wang,²⁸ G. Wang,²² J. Wang,⁵ M. J. Wang,²⁸ Q. F. Wang,²⁶ A. Warburton,¹¹ G. Watts,²⁵ T. Watts,²⁷ R. Webb,³⁰ C. Wei,⁶ C. Wendt,³⁴ H. Wenzel,¹⁴ W. C. Wester III,⁷ T. Westhusing,¹⁰ A. B. Wicklund,¹ E. Wicklund,⁷ R. Wilkinson,²¹

H. H. Williams,²¹ P. Wilson,⁵ B. L. Winer,²⁵ J. Wolinski,³⁰ D. Y. Wu,¹⁶ X. Wu,²² J. Wyss,²⁰ A. Yagil,⁷ W. Yao,¹⁴ K. Yasuoka,³² Y. Ye,¹¹ G. P. Yeh,⁷ P. Yeh,²⁸ M. Yin,⁶ J. Yoh,⁷ C. Yosef,¹⁷ T. Yoshida,¹⁹ D. Yovanovitch,⁷ I. Yu,³⁵ J. C. Yun,⁷ A. Zanetti,²² F. Zetti,²² L. Zhang,³⁴ S. Zhang,¹⁶ W. Zhang,²¹ and S. Zucchelli²

(CDF Collaboration)

- ¹Argonne National Laboratory, Argonne, Illinois 60439
²Istituto Nazionale di Fisica Nucleare, University of Bologna, I-40126 Bologna, Italy
³Brandeis University, Waltham, Massachusetts 02254
⁴University of California at Los Angeles, Los Angeles, California 90024
⁵University of Chicago, Chicago, Illinois 60637
⁶Duke University, Durham, North Carolina 27708
⁷Fermi National Accelerator Laboratory, Batavia, Illinois 60510
⁸Laboratori Nazionali di Frascati, Istituto Nazionale di Fisica Nucleare, I-00044 Frascati, Italy
⁹Harvard University, Cambridge, Massachusetts 02138
¹⁰University of Illinois, Urbana, Illinois 61801
¹¹Institute of Particle Physics, McGill University, Montreal, Canada H3A 2T8
and University of Toronto, Toronto, Canada M5S 1A7
¹²The Johns Hopkins University, Baltimore, Maryland 21218
¹³National Laboratory for High Energy Physics (KEK), Tsukuba, Ibaraki 305, Japan
¹⁴Lawrence Berkeley Laboratory, Berkeley, California 94720
¹⁵Massachusetts Institute of Technology, Cambridge, Massachusetts 02139
¹⁶University of Michigan, Ann Arbor, Michigan 48109
¹⁷Michigan State University, East Lansing, Michigan 48824
¹⁸University of New Mexico, Albuquerque, New Mexico 87131
¹⁹Osaka City University, Osaka 588, Japan
²⁰Università di Padova, Istituto Nazionale di Fisica Nucleare, Sezione di Padova, I-35131 Padova, Italy
²¹University of Pennsylvania, Philadelphia, Pennsylvania 19104
²²Istituto Nazionale di Fisica Nucleare, University and Scuola Normale Superiore of Pisa, I-56100 Pisa, Italy
²³University of Pittsburgh, Pittsburgh, Pennsylvania 15260
²⁴Purdue University, West Lafayette, Indiana 47907
²⁵University of Rochester, Rochester, New York 14627
²⁶Rockefeller University, New York, New York 10021
²⁷Rutgers University, Piscataway, New Jersey 08854
²⁸Academia Sinica, Taiwan 11529, Republic of China
²⁹Superconducting Super Collider Laboratory, Dallas, Texas 75237
³⁰Texas A&M University, College Station, Texas 77843
³¹Texas Tech University, Lubbock, Texas 79409
³²University of Tsukuba, Tsukuba, Ibaraki 305, Japan
³³Tufts University, Medford, Massachusetts 02155
³⁴University of Wisconsin, Madison, Wisconsin 53706
³⁵Yale University, New Haven, Connecticut 06511

(Received 9 August 1995)

We report on measurements of the $\Upsilon(1S)$, $\Upsilon(2S)$, and $\Upsilon(3S)$ differential, $(d^2\sigma/dP_t dy)_{y=0}$, and integrated cross sections in $p\bar{p}$ collisions at $\sqrt{s} = 1.8$ TeV using a sample of 16.6 ± 0.6 pb⁻¹ collected by the Collider Detector at Fermilab. The three resonances were reconstructed through the decay $\Upsilon \rightarrow \mu^+\mu^-$. Comparison is made to a leading order QCD prediction.

PACS numbers: 13.85.Ni, 12.38.Qk

We report a study of the reaction $p\bar{p} \rightarrow YX \rightarrow \mu^+\mu^-X$ at $\sqrt{s} = 1.8$ TeV. This study yields the P_t (momentum transverse to the beam direction) dependence of the production cross sections for the $\Upsilon(1S)$, $\Upsilon(2S)$, and $\Upsilon(3S)$ states, as well as the integrated cross sections. These results represent the first measurements of the individual Υ cross sections at a hadron collider and are important for the investigation of $b\bar{b}$ bound state production mechanisms in $p\bar{p}$ collisions [1–5]. It is expected that the Υ resonances are produced directly or from the decay of higher mass $b\bar{b}$ states. Using information from our silicon vertex detector, we have

previously determined [6] that $\Upsilon(1S)$ production is not consistent with the decay of long-lived particles. Since our measurements of prompt charmonia production for the J/ψ and $\psi(2S)$ states [7] are higher than the theoretical predictions [2,8,9], it is of interest to carry out similar comparisons for the Υ particles. Additionally, the Υ states allow exploration of the low P_t region inaccessible to the charmonia measurements, which do not extend below 4 GeV/c due to triggering constraints.

The data were collected in 1992–93 by the Collider Detector at Fermilab (CDF). The CDF detector has been described in detail elsewhere [10]. The components relevant

to this analysis are briefly described here. The z axis of the detector coordinate system is along the beam direction. The Central Tracking Chamber (CTC) is in a 1.4T axial magnetic field and has a resolution of $\delta P_t/P_t = \sqrt{(0.0011P_t)^2 + (0.0066)^2}$ for beam-constrained tracks where P_t is measured in GeV/c. The central muon chambers (CMU), at a radius of 3.5 m from the beam axis, are located behind five interaction lengths of calorimeter and provide muon identification in the region of pseudorapidity $|\eta| < 0.6$, where $\eta = -\ln[\tan(\theta/2)]$ and θ is the polar angle with respect to the beam axis. These chambers are complemented by the central muon upgrade system (CMP), which consists of four layers of drift chambers behind an additional four interaction lengths of steel absorber. Requiring the CMP reduces the hadronic punch-through backgrounds by approximately a factor of 10.

The measurements reported here are based on a $16.6 \pm 0.6 \text{ pb}^{-1}$ data sample of muon pairs collected with a three-level on-line trigger [11]. The level 1 trigger required two charged track segments in the central muon chambers. The efficiency for this trigger is 90% at $P_t = 3.1 \text{ GeV}/c$ and has a plateau of 94%. At level 2 at least one muon segment was required to match a CTC track found by a hardware track processor. The level 2 trigger is 90% efficient at $P_t = 3.1 \text{ GeV}/c$ and has a plateau of 93%. The level 3 trigger required a pair of fully reconstructed

tracks matched to hits in the muon chambers. Both muons were required to have P_t greater than 2.0 GeV/c, with at least one muon having P_t greater than 2.5 GeV/c.

Additional requirements were made off-line to isolate the Y resonances. Both muons from the $Y \rightarrow \mu^+ \mu^-$ decay were required to be identified by the CMU system and at least one muon had to be identified by the CMP system. The momenta of the muons were determined using CTC information along with the constraint that the particles must originate from the beam line. To reduce the sensitivity to the trigger thresholds, the P_t of both muons was required to be greater than 2.2 GeV/c and at least one muon had to have P_t greater than 2.8 GeV/c. Each muon chamber track was required to match its associated CTC track to within 3σ in $r - \phi$ and 3.5σ in z , where σ is the calculated uncertainty due to multiple scattering, energy loss, and measurement uncertainties. The muons were required to have opposite charge and the rapidity of the reconstructed pair had to be in the region $|y| < 0.4$, where $y = \frac{1}{2} \ln[(E + p_{\parallel})/(E - p_{\parallel})]$, E is the energy of the dimuon pair, and p_{\parallel} its momentum parallel to the beam direction. The resulting mass distribution of muon pairs, shown in Fig. 1, is well described by a fit to three Gaussians and a quadratic background.

The differential cross section times the branching ratio for $Y \rightarrow \mu^+ \mu^-$ is calculated in each P_t bin according to the equation

$$\left(\frac{d^2 \sigma(Y)}{dP_t dy} \right)_{y=0} B(Y \rightarrow \mu^+ \mu^-) = \frac{N_{\text{fit}}}{A \int \mathcal{L} dt \Delta P_t \Delta y \epsilon_{l1l2} \epsilon_{l3} \epsilon_{\text{trk}} \epsilon_{\text{rad}}},$$

where N_{fit} is the number of Y signal events in each P_t bin, A is the geometric and kinematic acceptance, $\int \mathcal{L} dt$

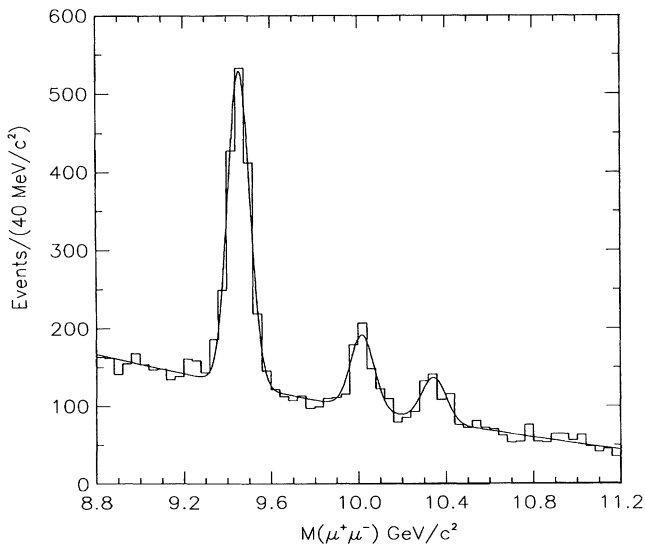


FIG. 1. The invariant mass distribution of muon pairs in the Y mass region for $|y| < 0.4$. The histogram corresponds to the data and the solid curve is a fit to three Gaussians plus a quadratic background.

is the integrated luminosity, ΔP_t is the width of the bin, and Δy is the rapidity range of the Y ($|y| < 0.4$). The various efficiency corrections include the combined level 1 and level 2 trigger efficiency ϵ_{l1l2} , the level 3 trigger efficiency ϵ_{l3} , the efficiency for reconstructing off-line both tracks in the CTC ϵ_{trk} and the efficiency for reconstructing both muon track segments and associating them with extrapolated CTC tracks ϵ_{μ} . The additional efficiency correction factor ϵ_{rad} accounts for event losses due to internal radiation from the muons.

A binned likelihood fit was performed on the dimuon mass distribution for each P_t bin to determine the number of signal events (N_{fit}). For the $Y(1S)$ the region between 8.7 and 9.8 GeV/c² was fit to a Gaussian plus quadratic background. In order to better estimate the background, the values of N_{fit} for the $Y(2S)$ and $Y(3S)$ were obtained by fitting all three resonances simultaneously to three Gaussians with a quadratic background. The Gaussian means were not fixed in these fits. The relative widths of the resonances in each P_t bin were constrained to values determined from Monte Carlo simulation. For the $Y(2S)$ and $Y(3S)$ resonances the region below P_t of 1 GeV/c is dominated by background and no significant excess of events was observed.

The geometric and kinematic acceptances for $Y(1S)$, $Y(2S)$, $Y(3S) \rightarrow \mu^+ \mu^-$ were calculated with a Monte

TABLE I. The differential cross section $(d^2\sigma/dP_t dy)_{y=0} \times B(Y(1S) \rightarrow \mu^+ \mu^-)$ for $Y(1S)$.

P_t bin GeV/c	Cross section pb/(GeV/c)	Stat. pb/(GeV/c)	Pol. Syst. pb/(GeV/c)		Other Syst. pb/(GeV/c)
			$\alpha = -1$	$\alpha = +1$	
0-0.5	31.0	± 7.9	-8.2	+5.9	± 3.5
0.5-1	64.6	± 11.2	-11.8	+6.9	± 7.3
1-2	96.2	± 10.0	-7.8	+1.7	± 10.9
2-3	130.1	± 11.8	+4.7	-2.4	± 14.7
3-4	106.2	± 10.9	+9.7	-5.0	± 12.0
4-5	100.3	± 10.8	+13.6	-5.6	± 11.4
5-6	74.3	± 9.4	+10.4	-3.7	± 8.4
6-7	53.5	± 7.9	+6.7	-2.5	± 6.1
7-8	37.8	± 6.7	+2.3	-0.4	± 4.3
8-9	26.0	± 5.5	-1.2	+0.1	± 2.9
9-10	27.6	± 5.0	-2.1	+0.7	± 3.1
10-12	15.2	± 2.7	-1.5	+0.9	± 1.7
12-16	5.6	± 1.1	-0.7	+0.5	± 0.6

TABLE II. The differential cross section $(d^2\sigma/dP_t dy)_{y=0} \times B(Y(2S) \rightarrow \mu^+ \mu^-)$ for $Y(2S)$.

P_t bin GeV/c	Cross section pb/(GeV/c)	Stat. pb/(GeV/c)	Pol. Syst. pb/(GeV/c)		Other Syst. pb/(GeV/c)
			$\alpha = -1$	$\alpha = +1$	
1-3	30.7	± 5.3	-1.1	+0.7	± 4.3
3-5	35.6	± 5.1	+3.6	-2.0	± 4.9
5-7	13.1	± 3.7	+1.9	-0.7	± 1.8
7-10	8.2	± 2.2	+0.5	-0.3	± 1.1

TABLE III. The differential cross section $(d^2\sigma/dP_t dy)_{y=0} \times B(Y(3S) \rightarrow \mu^+ \mu^-)$ for $Y(3S)$.

P_t bin GeV/c	Cross section pb/(GeV/c)	Stat. pb/(GeV/c)	Pol. Syst. pb/(GeV/c)		Other Syst. pb/(GeV/c)
			$\alpha = -1$	$\alpha = +1$	
1-3	21.3	± 4.5	-0.4	+0.7	± 3.0
3-5	15.9	± 4.3	+1.1	-1.0	± 2.2
5-10	5.4	± 1.8	+0.8	-0.3	± 0.8

Carlo simulation. The event generator produces Y particles with flat P_t and y distributions. Since the polarization of the Y resonances is not known, the states were assumed to decay isotropically. The generated events were processed with a detector simulation and with the same reconstruction criteria that were imposed on the data. The integrated acceptance A was computed for each P_t bin and varies in the range of 16% to 19%.

The events were corrected for the level 1 and level 2 trigger efficiency ϵ_{112} , which is typically 87% for each P_t bin. The values of the P_t independent efficiencies, determined from data, are $\epsilon_{13} = (92 \pm 2)\%$, $\epsilon_{\text{trk}} = (98 \pm 2)\%$, $\epsilon_{\mu} = (95 \pm 1)\%$, and $\epsilon_{\text{rad}} = (93 \pm 2)\%$.

A P_t dependent systematic uncertainty arises from the unknown Y polarization. This uncertainty was deter-

mined by recomputing the cross section assuming that the muons from the Y decay have an angular distribution proportional to $1 + \alpha \cos^2 \theta^*$, where θ^* is the polar angle in the rest frame of the Y and $\alpha = \pm 1$. The systematic uncertainty in the acceptance associated with the production model (7%) was determined by recalculating the acceptances using a parton level generator, which provides the four momenta of all known $b\bar{b}$ bound states which decay to the Y resonances [12]. The systematic uncertainty in the determination of N_{fit} [6% for $Y(1S)$ and 10% for the $Y(2S)$ and $Y(3S)$] was estimated by varying the Gaussian widths and the shape of the background used in the fits. Additional systematic uncertainties arise from the luminosity determination (3.6%), the level 1 and level 2 trigger efficiency

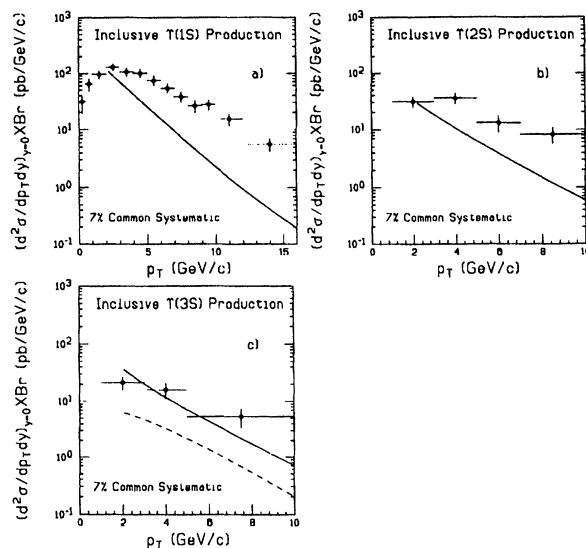


FIG. 2. (a) The product $(d^2\sigma/dp_T dy)_{y=0} \times B$ vs P_t for $Y(1S) \rightarrow \mu^+ \mu^-$. The vertical error bars include the statistical uncertainty added in quadrature with the polarization, fitting procedure, and acceptance model systematics. There is an additional common systematic of 7% from the efficiency corrections and luminosity determination that is not included in the error bars. The color-singlet calculation from Ref. [5], multiplied by $B(Y(1S) \rightarrow \mu^+ \mu^-) = 2.48\%$ [18] and divided by $\Delta y = 0.8$, is also shown. The theoretical prediction includes contributions from direct $Y(1S)$ production and $\chi_b(1P)$ and $\chi_b(2P)$ decay. (b) The product $(d^2\sigma/dp_T dy)_{y=0} \times B$ vs P_t for $Y(2S) \rightarrow \mu^+ \mu^-$. The indicated error bars are calculated as in (a). The color-singlet calculation from Ref. [5], multiplied by $B(Y(2S) \rightarrow \mu^+ \mu^-) = 1.31\%$ [18] and divided by $\Delta y = 0.8$, is also shown. The theoretical prediction includes contributions from direct $Y(2S)$ production and $\chi_b(2P)$ decay. (c) The product $(d^2\sigma/dp_T dy)_{y=0} \times B$ vs P_t for $Y(3S) \rightarrow \mu^+ \mu^-$. The indicated error bars are calculated as in (a). The color-singlet calculation from Refs. [5,13], multiplied by $B(Y(3S) \rightarrow \mu^+ \mu^-) = 1.81\%$ and divided by $\Delta y = 0.8$ is also shown. The dashed line corresponds to the direct $Y(3S)$ production contribution and the solid line corresponds to the sum of the contributions from the direct $Y(3S)$ production and the decay of the unobserved $\chi_b(3P)$ state.

corrections (4%), and the P_t independent efficiency corrections (4%).

The differential cross section results are summarized in Tables I–III. The asymmetric polarization systematic uncertainties are indicated separately from the other systematic uncertainties that have been added in quadrature. The results are displayed in Fig. 2 where the vertical error bars include the statistical uncertainty added in quadrature with the polarization, fitting procedure, and acceptance model systematic uncertainties. The common 7% systematic uncertainty associated with the efficiency corrections and the luminosity measurement is not included in the error bars.

Theoretical predictions from Ref. [5] are also shown in Fig. 2. These curves include only the color-singlet contributions discussed in Ref. [5] and are shown in the region $P_t > 2$ GeV/c, since below that value they are expected not to be reliable. The calculation for the $Y(1S)$

includes contributions from direct production and $\chi_b(1P)$ and $\chi_b(2P)$ decay [contributions from $Y(2S)$ and $Y(3S)$ decay are neglected]. The theoretical prediction for the $Y(2S)$ includes direct production and $\chi_b(2P)$ decay. Two theoretical curves are shown for the $Y(3S)$ cross section. One corresponds to the direct $Y(3S)$ production contribution [13] and the other to the sum of the contributions from the direct $Y(3S)$ production and the decay of the unobserved $\chi_b(3P)$ state. Recently attempts have been made to explain the discrepancies in both the shape and normalization between the theoretical and measured distributions. These include the inclusion of k_T effects [4] and novel color-octet production mechanisms [5,14]. These models are able to describe the data reasonably well. However, both rely on preliminary upsilon cross section results [15] to fix unknown parameters.

The integrated cross section results are

$$\begin{aligned} d\sigma/dy(\bar{p}p \rightarrow Y(1S), y = 0, 0 < P_t < 16 \text{ GeV}/c) \times B &= 753 \pm 29(\text{stat.}) \pm 72(\text{syst.}) \text{ pb}, \\ d\sigma/dy(\bar{p}p \rightarrow Y(2S), y = 0, 1 < P_t < 10 \text{ GeV}/c) \times B &= 183 \pm 18(\text{stat.}) \pm 24(\text{syst.}) \text{ pb}, \\ d\sigma/dy(\bar{p}p \rightarrow Y(3S), y = 0, 1 < P_t < 10 \text{ GeV}/c) \times B &= 101 \pm 15(\text{stat.}) \pm 13(\text{syst.}) \text{ pb}. \end{aligned}$$

The systematic uncertainties from the polarization model are 2%, 5%, and 5% for the $Y(1S)$, $Y(2S)$, and $Y(3S)$, respectively. The uncertainty from the acceptance model is estimated to be 3%. The uncertainty from the fitting procedure is conservatively taken to be the same as that used for the differential cross section values, as are the uncertainties from the luminosity determination and the efficiency corrections.

The ratios of the integrated cross section results can also be computed in the range $1 < P_t < 10$ GeV/c for $|y| < 0.4$. The results are $\sigma B(Y(2S))/\sigma B(Y(1S)) = 0.281 \pm 0.030(\text{stat.}) \pm 0.038(\text{syst.})$ and $\sigma B(Y(3S))/\sigma B(Y(1S)) = 0.155 \pm 0.024(\text{stat.}) \pm 0.021(\text{syst.})$. In calculating the systematic uncertainty on the ratio, the uncertainties arising from the fitting procedure, acceptance model, and assumed Y polarization were taken as uncorrelated. These production ratios are consistent with the results from experiments at lower energies [3,16].

In conclusion we have measured both the integrated and differential cross sections in the range $0 < P_t < 16$ GeV/c for the Y(1S) and in the range $1 < P_t < 10$ GeV/c for the Y(2S) and Y(3S) states. The rate of Y production was found to be higher than leading order QCD predictions [17]. Inclusion of additional production mechanisms may help to explain some of the discrepancies.

We thank the Fermilab staff and the technical staffs of the participating institutions for their vital contributions. This work was supported by the U.S. Department of Energy and National Science Foundation, the Italian Istituto Nazionale di Fisica Nucleare, the Ministry of Education, Science and Culture of Japan, the Natural Sciences and Engineering Research Council of Canada, the National Science Council of the Republic of China, and the A. P. Sloan Foundation.

*Visitor.

[1] R. Baier and R. Rückl, Z. Phys. C **19**, 251 (1983).

- [2] D. P. Roy and K. Sridhar, Phys. Lett. B **339**, 141 (1994).
- [3] R. Gavai *et al.*, Report No. CERN-TH.7526/94, 1994.
- [4] M. Mangano, Report No. CERN-TH.190/95, 1995.
- [5] P. Cho and A. K. Leibovich, Report No. CALT-68-1988, 1995.
- [6] H. Wenzel, Ph.D. thesis, Rheinisch-Westfälische Technische Hochschule Aachen, 1993.
- [7] F. Abe, *et al.*, Report No. Fermilab-Conf-94/136-E, 1994; Report No. Fermilab-Conf-95/226-E, 1995.
- [8] M. Cacciari and M. Greco, Phys. Rev. Lett. **73**, 1586 (1994).
- [9] E. Braaten *et al.*, Phys. Lett. B **333**, 548 (1994).
- [10] F. Abe *et al.*, Nucl. Instrum. Methods Phys. Res., Sect. A **271**, 387 (1988).
- [11] M. W. Bailey, Ph.D. thesis, Purdue University, 1994.
- [12] The parton level generator includes a $P_t - y$ correlation and calculates quarkonia production in $p\bar{p}$ collisions using matrix elements from Ref. [1] and from R. Gastmans, W. Troost, and T. T. Wu, Phys. Lett. B **184**, 257 (1987); Nucl. Phys. **B291**, 731 (1987).
- [13] P. Cho (private communication).
- [14] E. Braaten and S. Fleming, Phys. Rev. Lett. **74**, 3327 (1995).
- [15] F. Abe *et al.*, Report No. Fermilab-Conf-94/221-E, 1994.
- [16] K. Ueno *et al.*, Phys. Rev. Lett. **42**, 486 (1979); T. Yoshida *et al.*, Phys. Rev. D **39**, 3516 (1989); G. Moreno *et al.*, Phys. Rev. D **43**, 2815 (1991).
- [17] The D0 Collaboration has also presented preliminary values for the Y cross section, summed over the three resonances, in S. Abachi *et al.*, Report No. Fermilab-Conf-95/206-E, 1995.
- [18] Particle Data Group, Phys. Rev. D **50**, 1173 (1994).